I&EC research
Industrial & Engineering Chemistry Research

Article

pubs.acs.org/IECR

Alumina-Supported Nickel onto Cordierite Monoliths for Ethane Oxidehydrogenation: Coating Strategies and Their Effect on the Catalytic Behavior

Paula Brussino, Juan P. Bortolozzi, Viviana G. Milt, Ezequiel D. Banús, and María A. Ulla*

Instituto de Investigaciones en Catálisis y Petroquímica, INCAPE (FIQ, UNL-CONICET), Santiago del Estero 2829, 3000 Santa Fe, Argentina

ABSTRACT: Different strategies for the generation of Ni (15 wt %)/Al_2O_3 catalytic coatings onto cordierite monoliths applied to the oxidative dehydrogenation of ethane (ODHE) were investigated. Strategy 1 involved the deposition of an alumina layer (nanoparticles or micro + nanoparticles) and the later incorporation of the active phase. Strategy 2 employed a suspension containing a powder catalyst that was used to deposit the catalytic film. Morphological (SEM) and physicochemical (LRS and XPS) characterizations were used to explain the catalytic performance of the structured systems. The NiO particles' distribution on the obtained catalytic coatings was analyzed via SEM-EDX performed in different monolith regions. The ultrasonic test was used to evaluate the anchoring of these catalytic films to the substrates. It was concluded that the selection of both the strategy and the particle size of the support is extremely important to obtain a homogeneously dispersed, accessible, and highly adhered to the substrate catalyst.

1. INTRODUCTION

Ethylene is currently one of the most demanded compounds in the chemical industry due to its utility. It is used to manufacture polymers, ethylene oxide, styrene, ethylbenzene, oligomer products (e.g., alcohols, olefins), acetaldehyde, and vinyl acetate. The global demand for ethylene reached 139 million m.t. in 2014 and is forecast to grow up to 169 million m.t. by 2019.[1]

Steam cracking is actually a well-established industrial process for manufacturing ethylene, and the most used feedstocks are naphtha and ethane,[1] the latter being widely used in the U.S. After the recession of 2008−09, flexible steam crackers switched to ethane due to the low ethane price.[2] However, the steam cracking is also the most energy-consuming process in the chemical industry. Energy costs account for approximately 70% of production costs in typical ethane-, or naphtha-, based olefin plants.[2] These facts and the growing availability of cheaper alkanes from shale-gas have led us to explore alternative routes to produce ethene employing more energy-saving and less costly processes. An attractive pathway to produce ethylene is the oxidative dehydrogenation of ethane (ODHE) through a catalyst. This reaction is thermodynamically favored, and it can be carried out at relative low temperatures (300−500 °C) due to the presence of oxygen in the reagents stream and the generation of water as a byproduct.[3]

Several catalytic formulations in powder forms with variable ethylene yields have been studied.[4−9] Among them, the group of nickel-based catalysts has shown promising results in ethane conversion and ethylene selectivity. It has been reported that bulk nickel oxide is highly active for this reaction but also highly unselective, producing large amounts of carbon dioxide. This behavior is linked to the presence of unselective non-stoichiometric species of oxygen.[10−13] There are two approaches for reducing the amount of low selectivity species: the first one includes the incorporation of a high valence cation in the formulation, whereas the second one involves supporting the active phase onto a high surface area material.

Doping nickel oxide with a high valence cation is an attempt to modify the catalytic properties by reducing the amount of electrophilic oxygen radicals that are responsible for carbon dioxide production. The incorporation of niobium, cerium, tungsten, or tin has had positive effects on the ODH performance.[14−18] Recently, it has been reported that the incorporation of aluminum to the nickel oxide structure is beneficial for the catalytic behavior up to 30% wt.[19]

On the other hand, supported catalysts also present acceptable levels of selectivity and adequate yields of ethylene. A number of materials are employed as supports, but alumina has demonstrated its capacity to modify the electronic properties of nickel oxide, making it highly selective to ethylene.[10,20]

For all of these reasons, it is important to achieve a formulation capable of providing a satisfactory catalytic performance. However, if a commercial application were required, it would be mandatory to investigate the deposition of the catalysts onto a substrate. The assembly of a substrate (such as monoliths) and a catalyst constitutes a structured system that presents some advantages as compared to conventional fixed-bed reactors. These structured systems present high geometric surface area (using a packed bed, unrealistically small particles would be needed to achieve this), larger reactor productivities, better selectivity control, low-pressure drop, and higher efficiency. The runaway generated by hot spots is also minimized.[21]

Received: November 24, 2015
Revised: January 8, 2016
Accepted: January 26, 2016
Published: January 26, 2016

DOI: 10.1021/acs.iecr.5b04461
Ind. Eng. Chem. Res. 2016, 55, 1503−1512

Few articles have analyzed the use of structured catalysts for oxidehydrogenation; they have reported that an enhancement in the catalytic performance could be achieved with respect to powder forms.[22−25] The operation conditions and the materials employed as substrates exert influence on the final behavior of the catalytic systems. It has also been reported that the migration of certain components from the substrate (e.g., stainless steel) to the catalytic film could negatively affect the ethylene yield.[24,26] Cordierite monoliths are widely known as substrates to support oxidation catalysts used for the combustion of diesel soot.[27−30] Cordierite is a ceramic material that has very low expansion coefficient and high thermal stability. Such features make it an interesting material to be used as a substrate in a monolithic structure.

The aim of this work is to prepare homogeneous, Ni/Al_2O_3 thin film structured catalysts using cordierite monoliths as substrates and to study their physicochemical features and their catalytic performance on the oxidative dehydrogenation of ethane reaction. From an experimental approach, two different preparation strategies were explored to investigate their influence on the distribution and availability of the active species.

2. EXPERIMENTAL SECTION

2.1. Preparation of Structured Catalysts. The cordierite monoliths were provided by TENNECO and had 64 cells per square centimeter. The average wall thickness and average cell width were 150 and 1100 μm, respectively. The open frontal area is of 77%.[27] These were cut in pieces of 1 cm^2 in the front section and 2 cm in height. The cleaning procedure consisted of an ultrasonic bath in water for 30 min and then in acetone for 30 min. Finally, the monoliths were dried overnight at 130 °C in a stove and designated as Cor.

Two general procedures were used to prepare Ni/Al_2O_3 structured catalysts. In the first one, a γ-alumina coating was generated onto the monolith walls, and then, onto this film, the active phase was incorporated. In the second one, a suspension from a Ni/Al_2O_3 powder catalyst was deposited onto the channel walls of the monoliths. All samples prepared in this work contained a nominal value of 15% wt Ni (with respect to alumina).

These two procedures were based on the washcoating method via immersion-blowing-drying cycles. This method requires a solution (or suspension) with adequate properties (concentration of the precursor solution, rheological properties) to employ a sufficient number of cycles that allows one to obtain a homogeneous catalytic film with uniform distribution of the support and the active phase. In this sense, results obtained in our previous studies using ceramic monoliths[27] and other substrates[23,24,31] were taken into account to select the appropriate suspension requirement.

2.1.1. Strategy 1. Al_2O_3 Coating onto Monoliths: Al_2O_3(C)-Cor and Al_2O_3(S)-Cor. Two different alumina suspensions were employed to deposit the support coating with this procedure.

- Al_2O_3(C): Colloidal suspension (NYACOL 20% wt) with particle size of 50 nm, pH = 4, stabilized with HNO_3.
- Al_2O_3(S): Suspension composed of deionized water, poly(vinyl alcohol) (PVA), colloidal suspension of alumina (NYACOL 20% wt), and alumina powder (Puralox SBA-230, particle size of 45 μm), in a proportion of 3.15:0.09:1.12:1.

The alumina films were deposited onto the monoliths using cycles of immersion-blowing-drying via the washcoating method. The substrates were covered with Teflon tape and then with heat-shrinkable rubber to ensure the flow of suspension only through the channels. The substrates then were immersed into the corresponding suspension for 1 min, and later they were blown with an air pump for 30 s. After that, the structured substrates were dried in a stove for 1 h. The immersion-blowing-drying cycles were repeated until final weight was achieved. Finally, they were calcined at 550 °C for 2 h in a muffle furnace. After this stage, the samples were named as Al_2O_3(C)-Cor or Al_2O_3(S)-Cor.

Impregnation of the Active Components: Ni/Al_2O_3(C or S)-Cor. The active phase was incorporated into the alumina-coated monoliths using cycles of immersion-blowing-drying until the weight gain was around 15% wt of Ni. Finally, the samples were calcined at 550 °C for 2 h in a muffle. After this stage, the monoliths were designated as Ni/Al_2O_3(C)-Cor or Ni/Al_2O_3(S)-Cor, depending on the alumina suspension used as support in each case. For the immersion stage, a 0.43 M solution of nickel nitrate hexahydrate (SIGMA-Aldrich) was used, and the blowing time was the same as mentioned before. The cycles were repeated six times to prepare the Ni/Al_2O_3(C)-Cor samples and nine times for the other ones.

2.1.2. Strategy 2. Powder Catalyst Coating onto Monoliths: Ni/Al_2O_3(P)-Cor. A powder catalyst Ni/Al_2O_3(P) was prepared by conventional wet impregnation: γ-Al_2O_3 Puralox SBA-230 was used as support, and a nickel nitrate hexahydrate (SIGMA-Aldrich) solution was used as the active phase precursor. The amounts of each component were calculated to achieve 15% wt of Ni. The solvent was removed by evaporation, and the resulting powder was dried in a stove at 130 °C overnight. Once the catalyst was obtained, it was calcined in air flow at 550 °C for 4 h.

After that, a suspension (pH = 4) was prepared using the following proportions: H_2O:PVA:Al_2O_3:catalyst = 2.23:0.06:0.79:1. At this stage, the colloidal suspension of alumina was used as binder. The employed amounts were determined as optimal from previous studies.[31]

The catalyst coating was carried out using cycles of immersion-blowing-drying until the final loading of catalyst was achieved. The blowing time was 30 s. The samples then were calcined at 550 °C for 2 h and designated as Ni/Al_2O_3(P)-Cor.

2.2. Structured Catalyst Characterization. *X-ray Diffraction (XRD).* The X-ray diffractograms were obtained with a Shimadzu XD-D1 instrument with a monochromator using Cu Kα radiation at a scan rate of 2°/min, from 2θ = 20° to 80°. The monolith pieces were cut along the channels and held in a special holder for the XRD analysis.

X-ray Photoelectron Spectroscopy (XPS). Measurements were performed in a SPECS equipment with a hemispherical PHOIBOS150 analyzer operating in the FAT mode. The spectra were obtained with a pass energy of 30 eV and Mg Kα X-ray source power of 200 W. The samples were evacuated for 2 h in ultra high vacuum. The peak fitting was performed with the CASAXPS software, and C 1s at 284.6 was used as reference.

Scanning Electron Microscopy (SEM). A SEM Jeol JSM-35C equipment operated at 20 kV acceleration voltage was employed. Pieces of the different samples (structured substrate and catalyst) were prepared to examine the cross sections and

DOI: 10.1021/acs.iecr.5b04461
Ind. Eng. Chem. Res. 2016, 55, 1503−1512

inner channel walls. These portions were fixed to the sample holder and then coated with a gold thin layer.

Energy-Dispersive X-ray Analysis (EDX). The elemental chemical analysis was performed using the EDX system coupled to the SEM instrument. The results were obtained by the theoretical quantitative method (SEMIQ), which does not require standards.

The distribution of the Ni and Al in the catalytic layer was evaluated with a ZEISS instrument SUPRA 40 model, which was operated with an acceleration voltage of 20 kV. The apparatus was equipped with an EDS detector, Oxford Instruments, for EDX semiquantitative analysis. Also, a FEG (Field Emitter Gun) electron source was employed to study the elemental chemical composition and the elements distribution (mapping). Samples were glued to the sample holder with Ag painting. To improve the images quality, they then were coated with a thin layer of Pt.

Laser Raman Spectroscopy (LRS). The spectra were recorded using a LabRam spectrometer (Horiba-Jobin-Yvon) coupled to an Olympus confocal microscope (a 50× objective lens was used for simultaneous illumination and collection), equipped with a CCD detector cooled to about −70 °C using the Peltier effect. The excitation wavelength was in all cases 532.13 nm (Spectra Physics diode pump solid-state laser). The laser power was set at 30 mW.

Adherence Tests. A Testlab TB04 equipment (40 kHz and 160 W) was used to study the weight loss caused when the samples were exposed to an ultrasound bath. The samples were immersed into acetone, and they were submitted to ultrasound at 25 °C for 30 min. Three consecutive ultrasonic baths were performed.

Catalytic Tests. A flow system, operated between temperatures of 350−500 °C, was used. The feed composition was 6% C_2H_6, 6% O_2, and helium balance, with a W/F ratio fixed at 0.48 g s/cm^3. A second part of the experiments was carried out at fixed temperature (500 °C) but varying the W/F ratio to analyze the behavior of the selectivity with the conversion level.

3. RESULTS AND DISCUSSION

3.1. Synthesis of the Structured Catalysts. Figure 1 shows the weight gain of the structured supports after six cycles of immersion-blowing-drying for the Al_2O_3(C)-Cor monoliths and five cycles for the Al_2O_3(S)-Cor monoliths (Strategy 1). Figure 2 shows the weight gain corresponding to the incorporation of the active phase for the structured catalysts prepared with this procedure. Filled symbols represent the Ni precursor loading, while the unfilled ones belong to the active phase loading (after calcination). Figure 2a corresponds to the case where a commercial colloidal suspension of Al_2O_3 was used as a support, whereas Figure 2b belongs to the coatings deposited using an alumina suspension prepared in the laboratory.

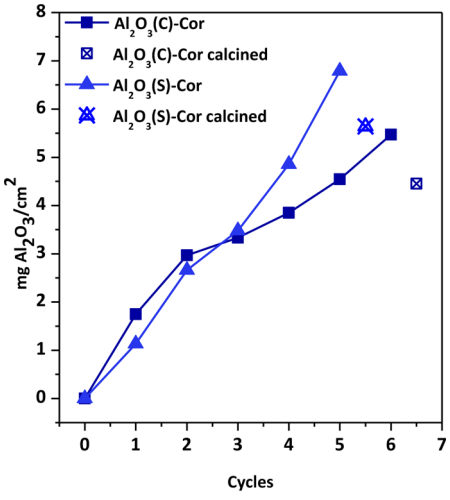

Figure 1. Weight gain per area of the structured supports (Strategy 1) as a function of the staged cycles.

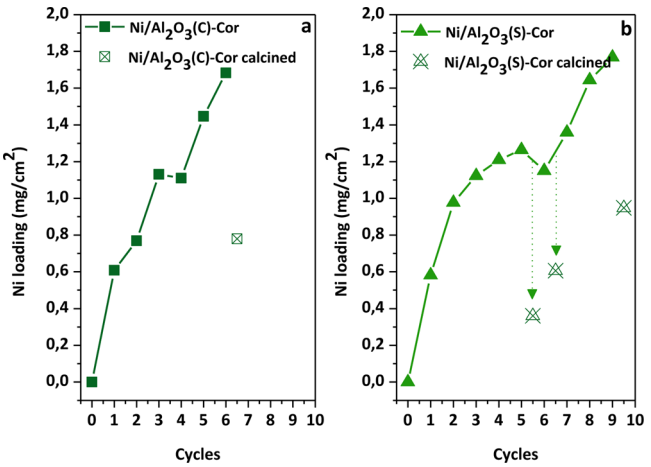

Figure 2. Incorporation of the active phase in Strategy 1 as a function of the staged cycles. (a) Ni/Al_2O_3(C)-Cor and (b) Ni/Al_2O_3(S)-Cor.

It is worth mentioning that the Ni/Al_2O_3(S)-Cor catalysts needed three additional cycles to achieve the same amount of active phase as compared to the Ni/Al_2O_3(C)-Cor monoliths. This behavior was related to the particle size of the support used in each case. When alumina nanoparticles were used (Ni/Al_2O_3(C)-Cor sample), the characteristic macropores of the cordierite were not completely sealed, so the nickel nitrate solution soaked these pores, allowing the precursor into them. On the other hand, when alumina microparticles were used, most of these pores were sealed and, hence, saturated with the nickel solution.

During the impregnation process, part of the nickel precursor (anchored to Al_2O_3) dissolved back into the nickel solution. Therefore, after the immersion step, no weight gain was obtained. This situation made intermediate calcination stages necessary for the Ni/Al_2O_3(S)-Cor monoliths (Figure 2b).

For Strategy 2, the generation of the catalytic layer with 15% wt of nickel required 4 cycles, with no intermediate calcinations (Figure 3).

3.2. Mechanical Stability of the Catalytic Layers. The structured catalysts were submitted to an ultrasound bath to study the adherence and interaction of the catalytic layer with the substrate. The tests were also carried out for the structured supports prepared by Strategy 1 (Al_2O_3(C)-Cor and Al_2O_3(S)-Cor).

Table 1 shows the adherence percentages with respect to the added layer, that is, excluding the cordierite monolith weight. Sample Al_2O_3(C)-Cor showed no significant differences in the adherence values with respect to the corresponding catalyst Ni/Al_2O_3(C)-Cor. The same situation was observed for Al_2O_3(S)-Cor. The addition of Ni slightly enhanced the adherence on both systems. After the impregnation of nickel nitrate, the samples were calcined, favoring the coating anchorage.

DOI: 10.1021/acs.iecr.5b04461
Ind. Eng. Chem. Res. 2016, 55, 1503−1512

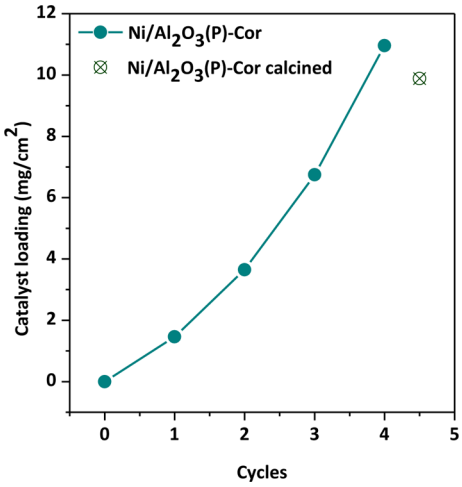

Figure 3. Incorporation of the catalyst in Strategy 2 as a function of the staged cycles.

Table 1. Adherences of the Supports and Catalytic Films to the Substrate

sample	% adherence
Al_2O_3(C)-Cor	92.60
Ni/Al_2O_3(C)-Cor	93.76
Al_2O_3(S)-Cor	95.77
Ni/Al_2O_3(S)-Cor	97.60
Ni/Al_2O_3(P)-Cor	98.09

The high adherence of the Ni/Al_2O_3(P)-Cor samples (98.09%) was similar to that of Ni/Al_2O_3(S)-Cor (97.60%). This could be related to the similar suspension recipe used to deposit the catalytic films. In both cases, the precursor suspensions contained micro- and nanoparticles. The presence of different particle sizes contributed to improve the particle−particle contact on the catalytic coating, promoting their cohesion and adhesion (Scheme 1).

3.3. Catalytic Performance of the Structured Catalysts. The prepared catalysts were tested in the ODHE reaction. The first part of the experiments was carried out under a fixed W/F ratio and an ethane/oxygen ratio of 1. Ethylene and carbon dioxide were the only products detected. Figure 4a shows the ethane conversion in the temperature range analyzed. The systems prepared with Strategy 1 (Ni/Al_2O_3(C)-Cor and Ni/Al_2O_3(S)-Cor) presented similar conversion values, whereas the one prepared from the powder catalyst (Ni/Al_2O_3(P)-Cor) exhibited low conversion, that is, 10% at the highest temperature. The highest ethane conversion was achieved by the Ni(15)/Al_2O_3(S)-Cor catalyst, around 29% at 500 °C.

A second part of tests was performed by varying the W/F ratio to obtain different conversion values at a fixed temperature, because the ethane conversion level can strongly affect the selectivity. The selectivity toward ethylene as a function of ethane conversion is shown in Figure 4b. With the increment of conversion, all prepared catalysts showed a decreasing trend, thus indicating that the overoxidation of ethylene occurred to some extent in all systems. However, the three evaluated catalysts behaved differently. The Ni/Al_2O_3(P)-Cor system showed the most marked decreasing trend, while the catalysts prepared by Strategy 1 evidenced a similar tendency: a lower drop with an increase in conversion. The monolith prepared from micrometric alumina with Strategy 1, Ni/Al_2O_3(S)-Cor, showed the highest selectivity in the conversion range analyzed, higher than 70% even at 30% of ethane conversion.

These observations are directly related to the morphological and physicochemical properties of the coatings. Their physicochemical characteristics and their distribution onto the substrate were investigated. The results are discussed below.

3.4. Phases and Morphology of the Catalytic Layers. The XRD patterns of the structured catalysts show that the prepared systems exhibit the characteristic peaks of cordierite (JCPDS-ICDD 12-303) and those of γ-Al_2O_3 (JCPDS-ICDD 47-1308) (Figure 5). The main diffraction peaks of NiO (JCPDS-ICDD 47-1049) at 2θ, 37.3°, 43.3°, and 62.9°, cannot be properly identified because they are overlapped by the cordierite and γ-Al_2O_3 signals. This observation could also indicate that crystallites with a few nanometers in size and that probably are amorphous were formed.

Scanning electron microscopy (SEM) coupled to energy dispersive X-ray analysis (EDX) was used to investigate the morphology and chemical composition of the coatings as well as the elements' distribution. It is necessary to remember that cordierite monoliths used in this work have macropores with sizes in the order of a few micrometers.

Different areas of each structured catalyst were analyzed. These areas are labeled as follows: "a" indicates a general view of the channel, "b" corresponds to the central area of this channel, "c" is related to a corner area, and "d" is associated with the monolith walls. Attached to each figure is displayed a

Scheme 1

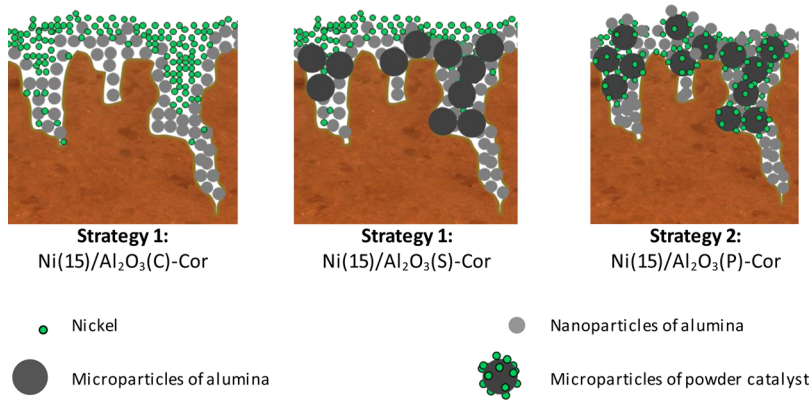

DOI: 10.1021/acs.iecr.5b04461
Ind. Eng. Chem. Res. 2016, 55, 1503−1512

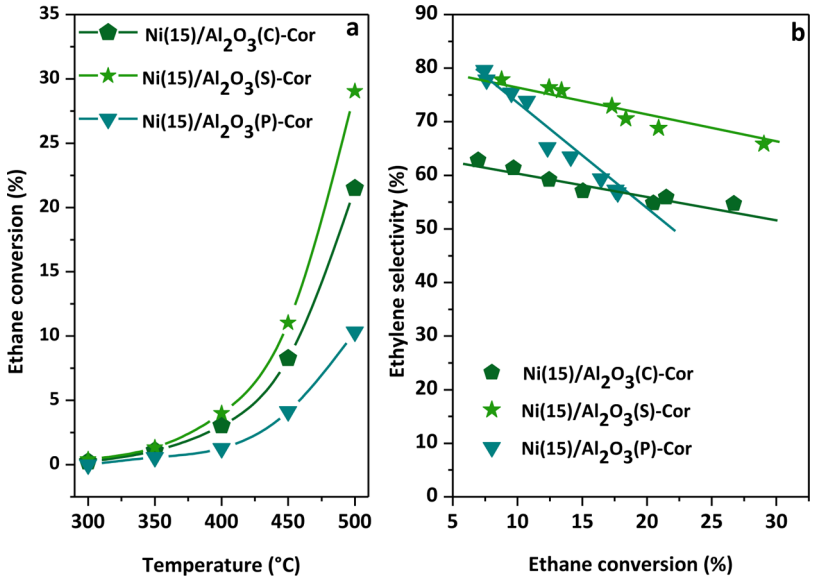

Figure 4. Catalytic performance of the structured catalysts. (a) Ethane conversion as a function of temperature, reaction conditions: W/F = 0.48 g·s/cm^3, C_2H_6/O_2 = 1. (b) Selectivity to ethylene at a fixed temperature; reaction conditions: T = 500 °C, W/F variable, and C_2H_6/O_2 = 1.

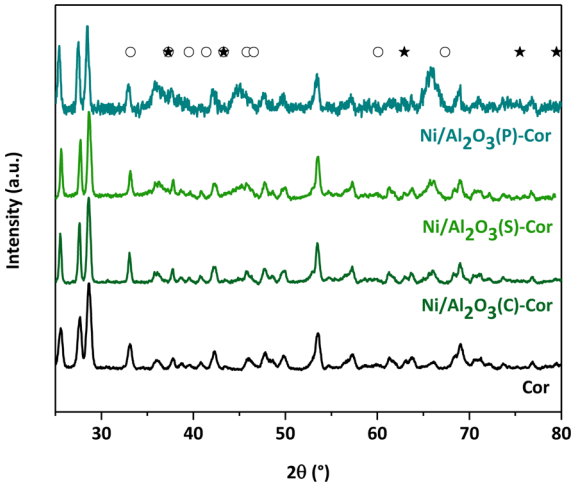

Figure 5. XRD patterns of the structured catalysts and cordierite. Symbols: ○, γ-Al_2O_3; ★, NiO.

table that shows the average atomic ratios of each element (relative to aluminum). The theoretical Mg/Al and Si/Al atomic ratios for the cordierite, 0.55 and 1.22, respectively, are taken as reference.

Figure 6 corresponds to the Ni/Al_2O_3(C)-Cor monolith. The obtained catalytic layer is smooth, and it covers a part of the wall macropores (Figure 6a and b). This fact is related to the alumina particle sizes used in this case (nanoparticles), which are smaller than the wall pore sizes. The EDX analysis in the central areas of the channel (Figure 6b) shows that the Mg/Al and Si/Al ratios, which are constitutive elements of the cordierite, are lower than those of the theoretical ratio. This indicates that the support particles got inside the macropores and that the catalytic film in those areas is less than 3 μm thick (EDX analysis depth). Values shown in Figure 6a and c are related to areas close to the walls, where the suspension is accumulated as a consequence of the fluid dynamic behavior of the system. In those cases, the values of Mg/Al and Si/Al are null, indicating that the catalytic layer is thicker than 3 μm. From these SEM images, the average film thickness was estimated to be between 15 and 30 μm (in the central area of the channels and close to the walls, respectively). Figure 6d shows the values corresponding to the Mg/Al and Si/Al in areas inside the walls. Particularly, a higher Si/Al ratio than that of the original cordierite was found. This could be explained by the fact that these cordierite monoliths are rich in silicon because in its manufacture process silica is added to the mixture as a binder. All of the elements under study were detected in this area, indicating that the alumina nanoparticles also got inside the walls, allowing the nickel precursor solution to infiltrate. Therefore, it is expected that a part of these NiO species are less accessible to the reactants. Besides, the macropores topology could also have retained some precursor solution during the blowing step, contributing to the growth of some bulk nickel oxide particles, which would have a negative effect on ethane selectivity (Figure 4b). It is well-known that bulk NiO promotes the direct oxidation of ethane to CO_2.[19,32] The Ni/Al ratio obtained for the different coating regions was 0.11 ± 0.01, indicating that Ni would be homogeneously distributed but, as said above, in the bulk form.

Figure 7 presents the results of the Ni/Al_2O_3(S)-Cor monoliths. It is worth recalling that this catalyst is mainly composed of micrometric particles of alumina as support. Figure 7a and b shows a rough catalytic layer that covers all cordierite macropores. The EDX results revealed that this layer is thicker than 3 μm in the central sector of the channels, unlike the previous system. The same results were obtained in regions close to the walls and corners (Figure 7a and c), where the values of Mg/Al and Si/Al ratios were equal to zero due to the accumulation of suspension in those areas as in the previous case. The estimated film thickness was around 20−30 μm. Inside the walls (Figure 7d), a higher Si/Al ratio than that of the original cordierite was also found, in agreement with what was explained above. It is worth noticing that the amount of Ni found in this area was lower than that of the previous system, in agreement with the SEM micrographs. In this case, the alumina particles are micrometric and they seal a larger amount of pores, in comparison with the alumina nanoparticles used in the Ni/Al_2O_3(C)-Cor systems. Consequently, in the Ni/Al_2O_3(S)-Cor catalysts, the support creates a "barrier", which prevents

DOI: 10.1021/acs.iecr.5b04461
Ind. Eng. Chem. Res. 2016, 55, 1503−1512

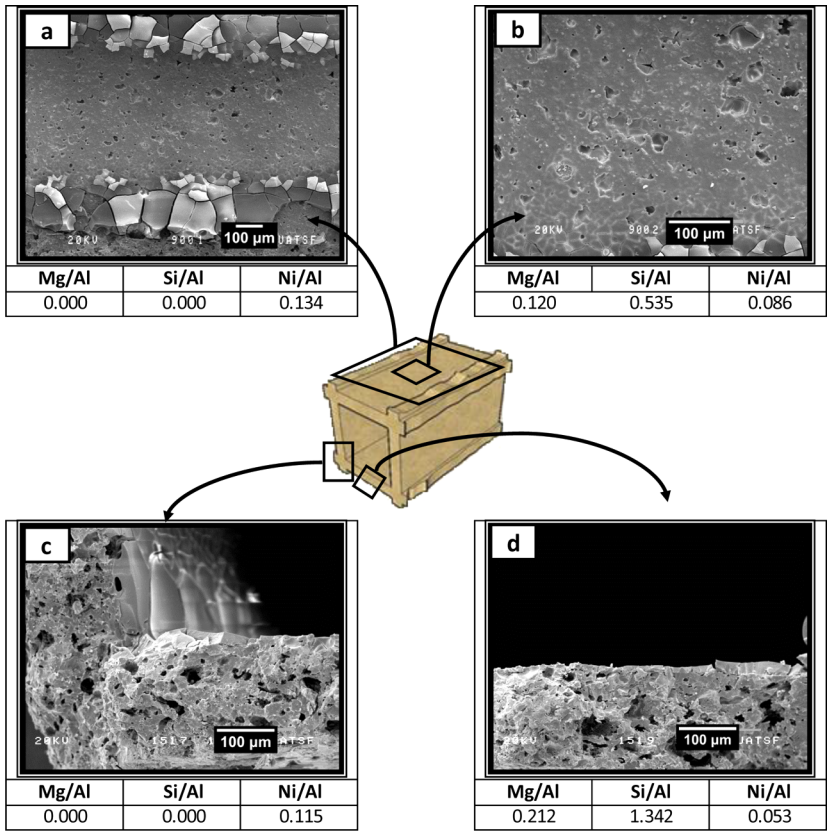

Figure 6. SEM micrographs and EDX results in different areas of Ni/Al_2O_3(C)-Cor. (a) General view of the channel, (b) central area of the channel, (c) corner area, and (d) monolith wall.

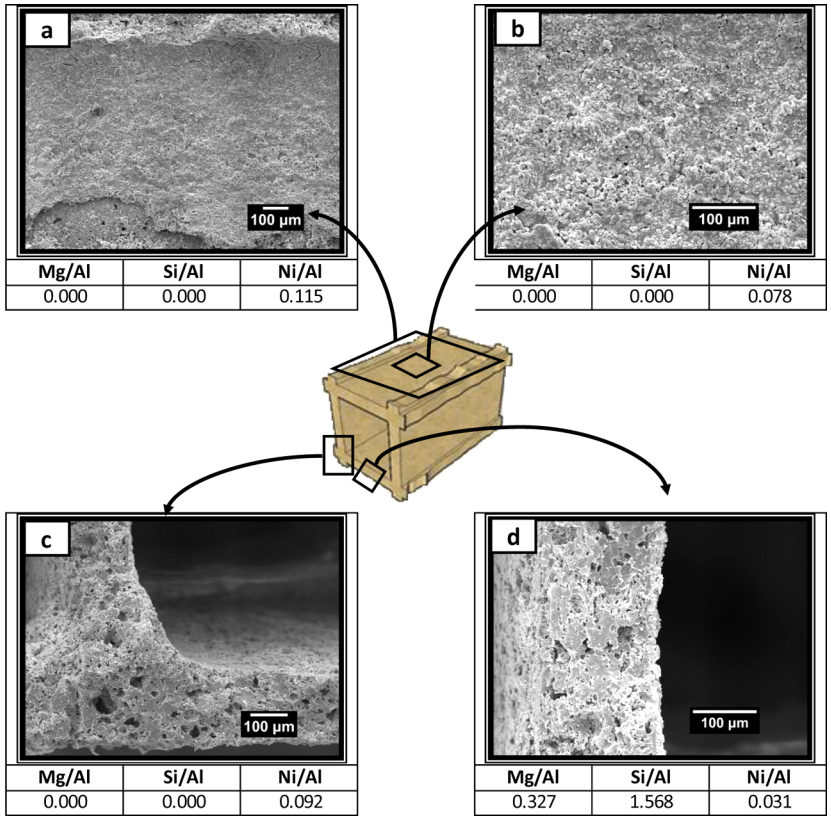

Figure 7. SEM micrographs and EDX results in different areas of Ni/Al_2O_3(S)-Cor. (a) General view of the channel, (b) central area of the channel, (c) corner area, and (d) monolith wall.

DOI: 10.1021/acs.iecr.5b04461
Ind. Eng. Chem. Res. 2016, 55, 1503−1512

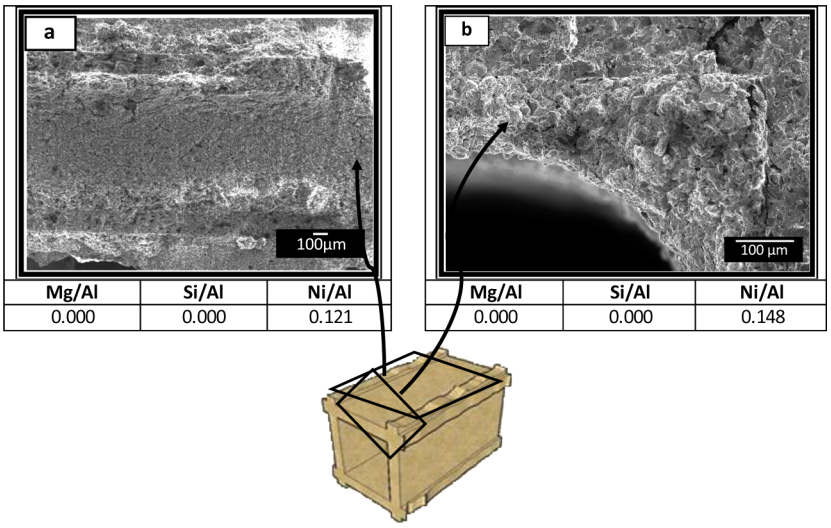

Figure 8. SEM micrographs and EDX results in different areas of Ni/Al_2O_3(P)-Cor. (a) Central area of the channel and (b) corner area.

the nickel introduction into the inner pores of the walls. Therefore, the Ni active species are more accessible to the reactants, in agreement with the increment of the catalytic activity observed for Ni/Al_2O_3(S)-Cor (Figure 4a). Besides, the Ni/Al ratio obtained in different coating regions was 0.09 ± 0.01, suggesting a homogeneous NiO particles' distribution on the support layer. This is consistent with the highest ethane selectivity achieved with this structured catalyst (Figure 4b).

Figure 8 presents SEM images and EDX results of the Ni/Al_2O_3(P)-Cor monoliths. The catalytic layer exhibits roughness as the previous system. As shown in this figure, the cordierite macropores have been completely sealed by the catalytic coating (Figure 8a and b). This is also noticed in the EDX results: in all areas examined in this sample, the Mg/Al and Si/Al ratios resulted null, also meaning that the film is thicker than 3 μm. The film thickness in this case is around 30 μm. A clear accumulation of catalyst in the corners of the channels was spotted. This accumulation is due to the fluidynamic behavior of the system.[33] Even though the coating topology is similar to that of Ni/Al_2O_3(S)-Cor and the Ni/Al ratio is higher than the ones obtained for the previous systems (compare Figures 6, 7, and 8a,b), the catalytic activity was lower and the ethane selectivity markedly decreased as the ethane conversion increased.

The overall distribution of the Ni and Al in the catalytic layer was evaluated by SEM-EDX mapping analysis. The Si and Mg mapping, both cordierite components, were also obtained for comparison. The component mapping of Ni/Al_2O_3(P)-Cor is shown in Figure 9. The same results were obtained with the other two samples (not shown). The images of Ni/Al_2O_3(P)-Cor system indicated an homogeneous distribution of Ni and Al onto the monolith channels. On the other hand, the distribution of Si and Mg shows uncovered cordierite areas (channel walls cut during the preparation for the analysis). The center of the images (inset) presents a picture of the analyzed zone, channels and walls of the structured catalyst.

3.5. NiO Species Characterization. Up to this point, the differences of the active sites between the structured catalysts prepared remain to be completely elucidated. LRS and XPS techniques can contribute to understanding these differences.

Figure 10 shows the Raman spectra for the Ni/Al_2O_3(C)-Cor and Ni/Al_2O_3(S)-Cor monoliths. Both samples present a

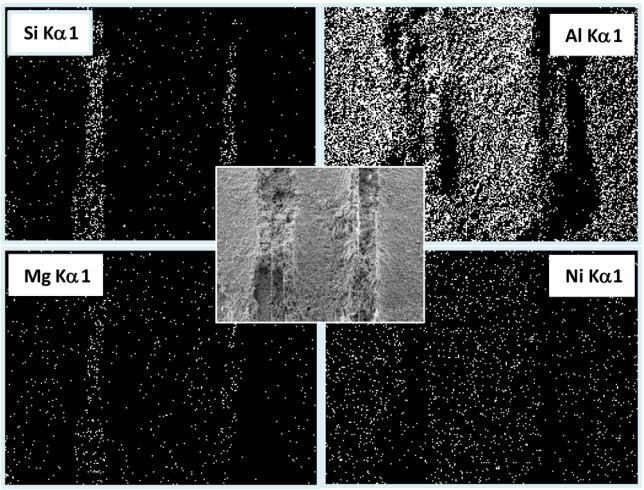

Figure 9. Ni, Al, Si, and Mg distribution on the channels and walls of Ni/Al_2O_3(P)-Cor.

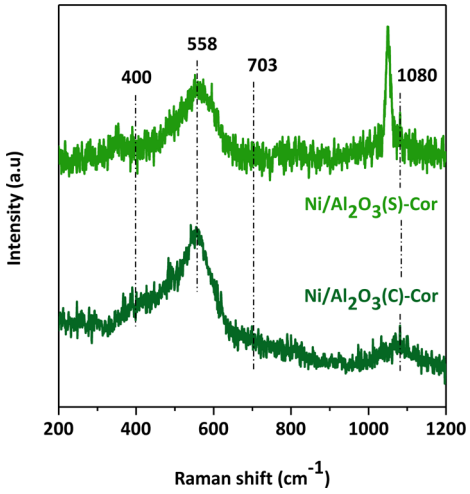

Figure 10. Laser Raman spectra of Ni/Al_2O_3(C)-Cor and Ni/Al_2O_3(S)-Cor.

broad and asymmetrical band centered at 557 cm^{-1} that corresponds to the Ni−O stretching mode. Bulk nickel oxide

DOI: 10.1021/acs.iecr.5b04461
Ind. Eng. Chem. Res. 2016, 55, 1503−1512

presents this band placed at 500 cm^{-1}. The shift of this signal to higher frequencies observed for the structured catalysts indicates a strong interaction of nickel species with the support.[23] A broad shoulder centered at ~400 cm^{-1} assigned to surface vacancies is also observed, suggesting the presence of small nonstoichiometric NiO particles. The weak signals at 700 and 1080 cm^{-1} are associated with second-order phononic modes. Particularly, the broad signal at 1080 cm^{-1} appears in both systems as a very weak band, indicating that NiO species are highly dispersed over the alumina surface.[34] Ni/Al_2O_3(S)-Cor monoliths present a strong signal at 1050 cm^{-1} possibly coming from the free nitrate species that remained on the surface after the Ni precursor decomposition.[35] Therefore, the NiO species on Ni/Al_2O_3(C)-Cor and Ni/Al_2O_3(S)-Cor are small NiO particles, highly dispersed with an important interaction with Al_2O_3. These species play a positive role as active sites for ODE.

Even though the Ni/Al ratio obtained by EDX for Ni/Al_2O_3(P)-Cor was the highest, the LRS spectrum of the former sample could not be obtained because of low signal intensities in the Ni−O stretching frequency region. The spectrum was taken in different areas of this catalytic coating with the same results, inferring the absence of large NiO particles. A possible scenario is that the initial NiO particles of the powder catalyst are hampered by the Al_2O_3 nanoparticles used as binder agent in Strategy 2. Therefore, the reactants would have low accessibility to the final NiO active sites on Ni/Al_2O_3(P)-Cor, resulting in a low ethane conversion (Figure 4a).

The surface analysis was performed by XPS (Figure 11). The Ni $2p_{3/2}$ main signals of the catalysts are positioned at higher

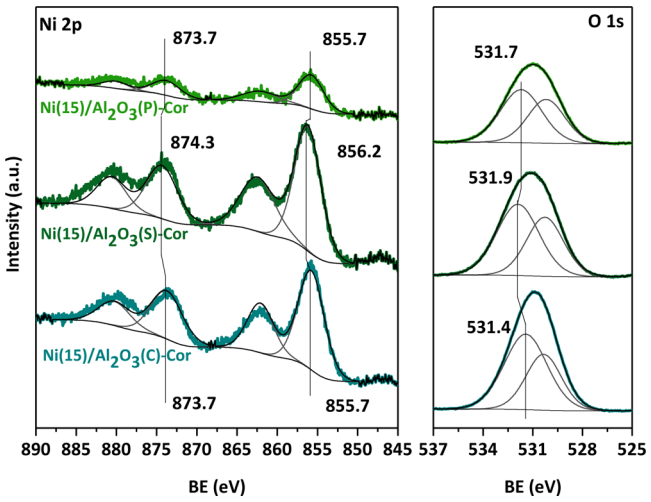

Figure 11. XPS spectra of the structured catalysts in the Ni 2p and O 1s regions.

binding energies (BE) than that of bulk NiO (854 eV), evidencing that Ni species are interacting with the support.[10,22,36] In addition, the difference in BE between the Ni $2p_{1/2}$ and Ni $2p_{3/2}$ was 18 eV for Ni(15)/Al_2O_3(C)-Cor and Ni(15)/Al_2O_3(P)-Cor, and it was 18.1 eV for Ni(15)/Al_2O_3(S)-Cor. These values are lower than those reported for bulk NiO (18.6 eV),[10] reinforcing the fact that there is a strong interaction between Ni species and alumina. These nickel species were proposed to be selective active sites on ethane oxidative dehydrogenation.[10,14,15,17,18,22−26]

Particularly, the Ni $2p_{3/2}$ BE of Ni(15)/Al_2O_3(S)-Cor catalyst shifted 0.5 eV to a higher BE with respect to that of the other ones, meaning that the former catalytic system had a higher NiO−support interaction, which is consistent with its better catalytic performance.

On the other hand, the Ni $2p_{3/2}$ BE of Ni(15)/Al_2O_3(P)-Cor is the same as that of Ni(15)/Al_2O_3(C)-Cor, suggesting the same NiO−Al_2O_3 surface interaction. However, the activity of the former catalyst was much lower than that of the latter one (Figure 4a). This behavior can be explained by a lower amount of surface NiO species on Ni(15)/Al_2O_3(P)-Cor. Its surface Ni/Al ratio, obtained from the XPS spectra, is around 3 times lower than that of Ni(15)/Al_2O_3(C)-Cor, and it was the lowest surface value found, confirming that the Al_2O_3 nanoparticles are on top of the catalyst particles hindering the active phase contact with the reactants. These nanoparticles were used as binder on the washcoating procedure. The Al_2O_3 increment on the outlayer of the catalytic coating not only hampers the NiO active sites decreasing the activity, but it also increases the Lewis and Brönsted acid sites, which favors ethene decomposition.[15,37] This could explain the marked drop in the selectivity of this system with the ethane conversion increment.

The O 1s spectrum presented two species of oxygen. One of them corresponds to lattice oxygen (O_L) from the NiO and alumina network. The other one at higher binding energy (O_V) could be related to carbonates, −OH, or oxygen atoms close to Ni vacancies. The BE of the oxygen species related to lattice oxygen is positioned at ~530.3 eV, in good agreement with the literature,[38−41] whereas the other oxygen species differs in the case of Ni(15)/Al_2O_3(C)-Cor. The O_V/O_L ratio in terms of area was calculated for the three catalysts. It was found that the Ni(15)/Al_2O_3(C)-Cor system has the highest value, and the other two systems have similar values. This could be related to the lower selectivity of this system (Figure 4b).

3.6. Summary of the Catalytic Coating Obtained (Scheme 1). Strategy 1, Ni(15)/Al_2O_3(C)-Cor: The catalytic coating obtained using Al_2O_3 nanoparticles in the central area of the channels is thin (<3 μm) because part of them are located inside the macropores. Besides, some NiO species are also formed there, and, consequently, they are unreachable for the reactants. The surface Ni species generated on the support outlayer are well distributed, resulting in an important Ni−Al_2O_3 interaction.

Strategy 1, Ni(15)/Al_2O_3(S)-Cor: The majority of the alumina particles are micrometric, sealing a large amount of the monolith wall pores and consequently generating a thick support layer. NiO species are well dispersed along the Al_2O_3 layer, also having a strong metal−support interaction, and more accessible to the reactants, improving their catalytic performance.

Strategy 2, Ni(15)/Al_2O_3(P)-Cor: The powder catalyst particles are micrometric and they generate a uniform coating, covering most of the monolith wall pores. However, some of the alumina nanoparticles seem to be placed on top of the catalytic coating, hampering NiO species and increasing the Lewis and Brönsted acid sites. This has a negative effect on the catalytic performance.

4. CONCLUSIONS

This study demonstrates that monolithic structured catalysts based on γ-Al_2O_3-supported NiO are active in the oxidative dehydrogenation of ethane reaction. The procedure used to generate the catalytic coating has a significant influence on the

DOI: 10.1021/acs.iecr.5b04461
Ind. Eng. Chem. Res. 2016, 55, 1503−1512

resulting catalytic behavior of these systems. If the macropores of the cordierite monoliths are not sealed, the active phase gets lost inside them, and therefore the catalysts lose activity.

On the other hand, preparing a suspension of the powder catalyst is not the best choice, with the NiO particles being "covered" by the binder agent (alumina) and, consequently, out of sight for the reactants. Furthermore, the exposure of alumina at the surface has a negative impact on the catalytic performance by enhancing the overoxidation of the produced olefin.

Therefore, the most appropriate method to generate a catalytic Ni/Al_2O_3 coating onto a cordierite monolith consists of two stages (Strategy 1) with a support composed of a mixture of micro- and nanoparticles of alumina. This system demonstrated to be a promising structured catalyst for the ODE reaction because it exhibits adequate ethane conversion and high selectivity to ethylene at a moderate temperature (500 °C).

Independent of the strategies discussed above, the three systems prepared showed significant adherence of the catalytic films to the substrate.

AUTHOR INFORMATION

Corresponding Author

*E-mail: mulla@fiq.unl.edu.ar.

Notes

The authors declare no competing financial interest.

ACKNOWLEDGMENTS

We acknowledge the financial support received from ANPCyT, CONICET, and UNL. Thanks are given to ANPCyT for the purchase of the SPECS multitechnique analysis instrument (PME8-2003) and the grant PME 87-PAE 36985 to purchase the RAMAN Instrument. Special thanks are also given to Ana Tarditi for her help in the XPS processing.

REFERENCES

(1) IHS Chemical Developments in Energy and Feedstock Markets and the Impact on Petrochemicals. T. Potter. Vice President, APAC − IHS Chemical Insight; http://www.apic2015.com/contents/downloads/2-2/1_IHS_Developments_in_Energy_and_Feedstock_Markets_and_the_Impact_on_Petrochemicals.pdf (accessed December 2015).

(2) Petrochemical Outlook Challenges and Opportunities. December 2014. EU-OPEC Energy Dialogue. https://ec.europa.eu/energy/sites/ener/files/documents/OPEC%20presentation.pdf (accessed December 2015).

(3) Ren, T.; Patel, M.; Blok, K. Olefins from conventional and heavy feedstocks: Energy use in steam cracking and alternative processes. *Energy* **2006**, *31*, 425.

(4) Zhu, H.; Dong, H.; Laveille, P.; Saih, Y.; Caps, V.; Basset, J. Metal oxides modified NiO catalysts for oxidative dehydrogenation of ethane to ethylene. *Catal. Today* **2014**, *228*, 58.

(5) Haddad, N.; Bordes-Richard, E.; Barama, A. MoOx-based catalysts for the oxidative dehydrogenation (ODH) of ethane to ethylene: Influence of vanadium and phosphorus on physicochemical and catalytic properties. *Catal. Today* **2009**, *142*, 215.

(6) Čapek, L.; Bulánek, R.; Adam, J.; Smoláková, L.; Sheng-Yang, H.; Čičmanec, P. Oxidative dehydrogenation of ethane over vanadium-based hexagonal mesoporous silica catalysts. *Catal. Today* **2009**, *141*, 282.

(7) Elbadawi, A. H.; Ba-Shammakh, M. S.; Al-Ghamdi, S.; Razzak, S. A.; Hossain, M. M. Reduction kinetics and catalytic activity of VO_x/γ-Al_2O_3-ZrO_2 for gas phase oxygen free ODH of ethane. *Chem. Eng. J.* **2016**, *284*, 448.

(8) Heracleous, E.; Machli, M.; Lemonidou, A. A.; Vasalos, I. A. Oxidative dehydrogenation of ethane and propane over vanadia and molybdena supported catalysts. *J. Mol. Catal. A: Chem.* **2005**, *232*, 29.

(9) Che-Galicia, G.; Quintana-Solórzano, R.; Ruiz-Martínez, R. S.; Valente, J. S.; Castillo-Araiza, C. O. Kinetic modeling of the oxidative dehydrogenation of ethane to ethylene over a MoVTeNbO catalytic system. *Chem. Eng. J.* **2014**, *252*, 75.

(10) Heracleous, E.; Leeb, A. F.; Wilson, K.; Lemonidou, A. A. Investigation of Ni-based alumina-supported catalysts for the oxidative dehydrogenation of ethane to ethylene: structural characterization and reactivity studies. *J. Catal.* **2005**, *231*, 159.

(11) Savova, B.; Loridant, S.; Filkova, D.; Millet, J. M. M. Ni−Nb−O catalysts for ethane oxidative dehydrogenation. *Appl. Catal., A* **2010**, *390*, 148.

(12) Skoufa, Z.; Heracleous, E.; Lemonidou, A. A. On ethane ODH mechanism and nature of active sites over NiO-based catalysts via isotopic labeling and methanol sorption studies. *J. Catal.* **2015**, *322*, 118.

(13) Heracleous, E.; Lemonidou, A. A. Ni−Nb−O mixed oxides as highly active and selective catalysts for ethene production via ethane oxidative dehydrogenation. Part II: Mechanistic aspects and kinetic modelling. *J. Catal.* **2006**, *237*, 175.

(14) Heracleous, E.; Lemonidou, A. A. Ni−Me−O mixed metal oxides for the effective oxidative dehydrogenation of ethane to ethylene − Effect of promoting metal Me. *J. Catal.* **2010**, *270*, 67.

(15) Solsona, B.; López Nieto, J. M.; Concepción, P.; Dejoz, A.; Ivars, F.; Vázquez, M. I. Oxidative dehydrogenation of ethane over Ni−W−O mixed metal oxide catalysts. *J. Catal.* **2011**, *280*, 28.

(16) Skoufa, Z.; Heracleous, E.; Lemonidou, A. A. Unraveling the contribution of structural phases in Ni−Nb−O mixed oxides in ethane oxidative dehydrogenation. *Catal. Today* **2012**, *192*, 169.

(17) Solsona, B.; Concepción, P.; Demicol, B.; Hernández, S.; Delgado, J. J.; Calvino, J. J.; López Nieto, J. M. Selective oxidative dehydrogenation of ethane over SnO_2-promoted NiO catalysts. *J. Catal.* **2012**, *295*, 104.

(18) Solsona, B.; Concepción, P.; Hernández, S.; Demicol, B.; López Nieto, J. M. Oxidative dehydrogenation of ethane over NiO−CeO_2 mixed oxides catalysts. *Catal. Today* **2012**, *180*, 51.

(19) Skoufa, Z.; Xantri, G.; Heracleous, E.; Lemonidou, A. A. A study of Ni−Al−O mixed oxides as catalysts for the oxidative conversion of ethane to ethylene. *Appl. Catal., A* **2014**, *471*, 107.

(20) Čapek, L.; Vaněk, L.; Adam, J.; Smoláková, L. Dehydrogenation of ethane over vanadium, cobalt and nickel based catalysts. *Stud. Surf. Sci. Catal.* **2008**, *174B*, 1175.

(21) Moulijn, J. A.; Stankewickz, A.; Kapteijn, F. The potential of structured reactors in process intensification. *Chem. Sustainable Dev.* **2003**, *11*, 3−9.

(22) Chu, B.; Truter, L.; Nijhuis, T. A.; Cheng, Y. Oxidative dehydrogenation of ethane to ethylene over phase-pure M1MoVNbTeOx catalysts in a micro-channel reactor. *Catal. Sci. Technol.* **2015**, *5*, 2807.

(23) Bortolozzi, J. P.; Gutierrez, L. B.; Ulla, M. A. Efficient structured catalysts for ethylene production through the ODE reaction: Ni and Ni−Ce on ceramic foams. *Catal. Commun.* **2014**, *43*, 197.

(24) Bortolozzi, J. P.; Weiss, T.; Gutierrez, L. B.; Ulla, M. A. Comparison of Ni and Ni−Ce/Al_2O_3 catalysts in granulated and structured forms: Their possible use in the oxidative dehydrogenation of ethane reaction. *Chem. Eng. J.* **2014**, *246*, 343.

(25) Bortolozzi, J. P.; Banús, E. D.; Milt, V. G.; Miro, E. E. New formulations of Ni-containing ceramic papers to enhance the catalytic performance for the oxidative dehydrogenation of ethane. *Ind. Eng. Chem. Res.* **2014**, *53*, 17570.

(26) Löfberg, A.; Giornelli, T.; Paul, S.; Bordes-Richard, E. Catalytic coatings for structured supports and reactors: VO_x/TiO_2 catalyst coated on stainless steel in the oxidative dehydrogenation of propane. *Appl. Catal., A* **2011**, *391*, 43.

(27) Banús, E. D.; Milt, V. G.; Miro, E. E.; Ulla, M. A. Catalytic coating synthesized onto cordierite monolith walls. Its application to diesel soot combustion. *Appl. Catal., B* **2013**, *132−133*, 479.

DOI: 10.1021/acs.iecr.5b04461
Ind. Eng. Chem. Res. 2016, 55, 1503−1512

(28) Neyertz, C. A.; Banús, E. D.; Miró, E. E.; Querini, C. A. Potassium-promoted $Ce_{0.65}Zr_{0.35}O_2$ monolithic catalysts for diesel soot combustion. *Chem. Eng. J.* **2014**, *248*, 394.
(29) Soloviev, S. O.; Kapran, A. Y.; Kurylets, Y. P. Oxidation of diesel soot on binary oxide CuCr(Co)-based monoliths. *J. Environ. Sci.* **2015**, *28*, 171.
(30) Gálvez, M. E.; Ascaso, S.; Tobías, I.; Moliner, R.; Lázaro, M. J. Catalytic filters for the simultaneous removal of soot and NO_x: Influence of the alumina precursor on monolith washcoating and catalytic activity. *Catal. Today* **2012**, *191*, 96.
(31) Banús, E. D.; Sanz, O.; Milt, V. G.; Miro, E. E.; Montes, M. Development of a stacked wire-mesh structure for diesel soot combustion. *Chem. Eng. J.* **2014**, *246*, 353.
(32) Heracleous, E.; Lemonidou, A. A. Ni−Nb−O mixed oxides as highly active and selective catalysts for ethene production via ethane oxidative dehydrogenation. Part I: Characterization and catalytic performance. *J. Catal.* **2006**, *237*, 162.
(33) Kolb, W. B.; Papadimitriou, A. A.; Cerro, R. L.; Leavitt, D. D.; Summers, J. C. The ins and outs of coating monolithic structures. *Chem. Eng. Prog.* **1993**, *89*, 61.
(34) Yisup, N.; Cao, Y.; Feng, W.; Dai, W.; Fan, K. Catalytic oxidation of methane over novel Ce−Ni−O mixed oxide catalysts prepared by oxalate gel-coprecipitation. *Catal. Lett.* **2005**, *99*, 207.
(35) Jentzsch, P. V.; Ciobotă, V.; Bolanz, R. M.; Kampe, B.; Rösch, P.; Majzlan, J.; Popp, J. Raman and infrared spectroscopic study of synthetic ungemachite $K_3Na_8Fe(SO_4)_6(NO3)_2.6H_2O$. *J. Mol. Struct.* **2012**, *1022*, 147.
(36) Kirumakki, S. R.; Shpeizer, B. G.; Sagar, G. V.; Chary, K. V. R.; Clearfield, A. Hydrogenation of Naphthalene over $NiO/SiO_2-Al_2O_3$ catalysts: Structure−activity correlation. *J. Catal.* **2006**, *242*, 319.
(37) López Nieto, J. M.; Solsona, B.; Grasselli, R. K.; Concepción, P. Promoted NiO Catalysts for the Oxidative Dehydrogenation of Ethane. *Top. Catal.* **2014**, *57*, 1248.
(38) Preda, I.; Mossanek, R. J. O.; Abbate, M.; Alvarez, L.; Méndez, J.; Gutiérrez, A.; Soriano, L. Surface contributions to the XPS spectra of nanostructured NiO deposited on HOPG. *Surf. Sci.* **2012**, *606*, 1426.
(39) Kitakatsu, N.; Maurice, V.; Hinnen, C.; Marcus, P. Surface hydroxylation and local structure of NiO thin films formed on Ni(111). *Surf. Sci.* **1998**, *407*, 36.
(40) Langell, M. A.; Berrie, C. L.; Nassir, M. H.; Wulser, K. W. Adsorption of acetic acid on hydroxylated NiO(111) thin fllms. *Surf. Sci.* **1994**, *320*, 25.
(41) Paynea, B. P.; Biesinger, M. C.; McIntyre, N. S. Use of oxygen/nickel ratios in the XPS characterization of oxide phases on nickel metal and nickel alloy surfaces. *J. Electron Spectrosc. Relat. Phenom.* **2012**, *185*, 159.

DOI: 10.1021/acs.iecr.5b04461
Ind. Eng. Chem. Res. 2016, 55, 1503−1512